Applied Catalysis B: Environmental 221 (2018) 664–669

Contents lists available at ScienceDirect

Applied Catalysis B: Environmental

journal homepage: www.elsevier.com/locate/apcatb

Research paper

Use of aligned triphenylamine-based radicals in a porous framework for promoting photocatalysis

Yan-Xi Tan, Yan-Ping He, Daqiang Yuan*, Jian Zhang*

State Key Laboratory of Structural Chemistry, Fujian Institute of Research on the Structure of Matter, Chinese Academy of Sciences, Fuzhou, 350002, PR China

ARTICLE INFO

Keywords:
Metal-organic framework
Triphenylamine-based radical
Photoinduced electron transfer
Heterogeneous catalyst
Mannich photocatalysis

ABSTRACT

The Ca-MOF **FIR-29** is synthesized and exhibits a honeycomb lattice of hexagonal channels with an aperture of ~16 Å, giving a BET surface area of 2061 $m^2 g^{-1}$. The consecutive slipped π···π stacking interactions of photoactive tris((4-carboxyl)phenylduryl)amine (TCPA) groups on the surface of hexagonal channels makes it an effective photocatalyst for catalyzing the typical Mannich photocatalysis, forming *β*-tetrahydroisoquinolne ketones in high isolated yields. Catalytic activity for **FIR-29** is about 2.7 times enhancement over that for mesoporous DUT-63 consisted of discrete TCPA groups without any intermolecular interaction. This is mainly due to the fact that the rigid compact stacking of tri([1,1′-biphenyl]-4-yl)amine (TBPA) is conducive to form stable TBPA radical, and is optimal for electron or energy transfer to expedite the reactivity of sp^3 carbon atoms and allow higher photocatalytic conversion.

Dedicated to professor Xin[HYPHEN]Tao Wu on the occasion of his 80th

1. Introduction

In the past decades, visible-light-driven photocatalysis as an eco-friendly and energy-efficient method for organic synthesis has been extensively explored [1–6]. Compared with traditional noble metal photocatalysts, organic dyes have recently attracted much attention of synthetic chemists because their promising characteristics of efficient visible-light absorption, enhanced stability, and modification susceptibility promote their application in photocatalysis [7–14]. For example, triphenylamine (TPA) and its derivatives have excellent hole-transport properties and have been widely used to construct hole-transport materials for efficient photoredox reactions [15,16]. However, the homogeneous catalysis of these TPA-based complexes makes their recycling and products separation difficult, which will further delay their practical applications in photocatalytic processes [17]. An effective approach to resolve this issue centers is to trap these TPA-based complexes into porous solid materials, making easy catalysts reuse and products purification [18–23].

Metal-organic frameworks (MOFs) are interesting hybrid solids with ordered infinite networks consisting of organic bridging ligands and inorganic nodes [24–32]. The unique porous structure of MOFs encapsulating photoactive organic groups allows them to demonstrate considerable promise in photocatalysis [26,33–42]. Recently, to overcome the current limitation of visible-light-driven photocatalysis and enhance photocatalytic conversion of poorly active chemical bonds in organic synthesis, a significant consecutive photoinduced electron transfer (conPET) process[43] of the perylene diimide (PDI) radical anion was applied to a Zn-PDI MOF for the reduction of aryl halides [33]. Although TPA derivatives can't perform such conPET process similar to PDI units, long-range π···π stacking of TPA derivatives with conjugated systems, such as tri([1,1′-biphenyl]-4-yl)amine (TBPA), can support some favorable factors for photocatalysis, including 1) the formation of stable radical with high local concentration; 2) a strong attraction to aromatic substrate molecules; 3) their packing state being optimal for electron or energy transfer [33]. These favorable factors endow desirable photocatalysis potential of TPA derivatives. Especially, the incorporation of well-organized TBPA fragments into MOFs represents a promising approach to heterogenize these photoconversions and to overcome the restrictions of the homogeneous process. Tris((4-carboxyl)phenylduryl)amine (H_3TCPA), a trigonal ligand that contains the photoactive TBPA group, has been employed to build some MOFs used for their gas sorption and optical properties [44–48], but none of them shows visible-light-driven photocatalysis in organic synthesis, because the TBPA units in these MOFs were not aligned appropriately.

In this paper, the redox-active Ca-MOF, $(\{[Ca_5(TCPA)_3(H_2O)_6]^+\}_n \cdot nNO_3^-$, **FIR-29**, FIR denotes Fujian Institute of Research) shows hexagonal channels with an aperture of 16 Å and well-organized aggregation of photoactive TBPA moieties as aryl radicals, making it an effective photocatalyst. The typical oxidative Mannich reaction[49] of *N*-phenyltetrahydroisoquinoline and

* Corresponding author.
E-mail addresses: ydq@fjirsm.ac.cn (D. Yuan), zhj@fjirsm.ac.cn (J. Zhang).

http://dx.doi.org/10.1016/j.apcatb.2017.09.054
Received 10 August 2017; Received in revised form 19 September 2017; Accepted 23 September 2017
Available online 23 September 2017
0926-3373/

nonactivated ketones under mild conditions is selected as model substrates to examine the feasibility of the optimal photoinduced electron transfer (PET) process in the consecutive long-range π···π stacking of the stable TBPA radials.

2. Experimental

2.1. Materials and methods

Commercially available reagents were used as received. Thermal gravimetric analysis data were obtained with an NETZSCH STA 449C analyzer. All samples and reference (Al_2O_3) were enclosed in a platinum crucible and were heated from 25 to 700 °C at a rate of 10 °C/min under an N_2 atmosphere. X-ray powder diffraction (XRPD) patterns were collected on a Rigaku Mini 600 X-ray diffractometer with Cu Kα radiation (λ = 1.5406 Å) at a scanning rate of 5°/min for 2θ ranging from 4° to 40°. Simulated XRPD patterns were calculated using Mercury from corresponding single-crystal structural models. ^{1}H NMR spectra were recorded on a Bruker Avance 400 (400.1 MHz for ^{1}H NMR). The deuterated solvents used are indicated in the experimental part. EPR spectra were recorded on a Bruker BioSpin E500 EPR spectrometer with a 100 kHz magnetic field modulation at room temperature equipped with a 16 mW ultraviolet lamp. Gas adsorption measurement was performed in the ASAP 2020 System. Optical diffuse reflectance spectra were measured at room temperature on a Perkin Elmer Lambda-950 UV/Vis/NIR spectrophotometer by using $BaSO_4$ as baseline sample.

2.2. Preparation of $\{[Ca_5(TCPA)_3(H_2O)_6]^+\}_n \cdot nNO_3^-$ (FIR-29)

H_3TCPA (60 mg), $Ca(NO_3)_2 \cdot 4H_2O$ (50 mg), 4 mL dimethylacetamide (DMA) and 0.5 mL H_2O in an 8 mL vial was stirred for 30 min, and then sealed and heated in an oven at 120 °C for 3 days. The vial was then cooled to room temperature. After washing with fresh DMA, yellow triangular-prism-shaped crystals were obtained in pure form (Yield: 70 mg, 57% based on H_3TCPA).

2.3. X-ray crystallography

The diffraction data of **FIR-29** was collected on a SuperNova diffractometer equipped with a copper micro-focus X-ray sources (λ = 1.5406 Å) and an Atlas CCD detector under 100 K. Empirical absorption correction used spherical harmonics, implemented in SCALE3 ABSPACK scaling algorithm. The structure was solved by direct methods and refined with full-matrix least-squares technique using *SHELXL*-2014. All non-hydrogen atoms were refined with anisotropic displacement parameters. The diffused electron densities resulting from these residual solvent molecules were removed from the dataset using the *SQUEEZE* routine of *PLATON* and refined further using the data generated. The contents of the solvent region are not represented in the unit cell contents in the crystal data. Crystal data of **FIR-29**: $C_{117}H_{72}N_3O_{24}Ca_5$, Mr = 2104.17, space group $P3_121$, a = 37.0787(5) Å, c = 30.0922(7) Å, V = 35828.9(13) Å^3, Z = 6, D_c = 0.585 g cm^{-3}, F_{000} = 6522, CuKα radiation, λ = 1.54184 Å, T = 100.0(2) K, 48768 reflections collected, 29178 unique (R_{int} = 0.0757). Final GooF = 1.095, $R1$ = 0.0894, $wR2$ = 0.2211, R indices based on 6522 reflections with ($I > 2\sigma(I)$) (refinement on F^2).

2.4. Typical experimental procedure for catalysis

Representative procedure: to a 10 mL Schleck flask equipped, crystalline powder of **FIR-29** (5.0 mmol% based on Ca_5 cluster), the respective substrate (0.5 mmol) and L-proline (6 mg) were added into dry MeCN (3 mL) and acetone (1 mL) via stirring. Then the reaction mixture was stirred under open air for 8 h at a distance of about 5 cm from a 7 W blue LEDs lamp. Upon the completion of reaction, as monitored by TLC (petroleum ether: ethyl acetate = 4:1), the crude reaction mixture was purified by flash chromatography on silica gel (silica: 200–300 mesh; eluent: petroleum ether/ethyl acetate (4:1) to provide the corresponding pure product.

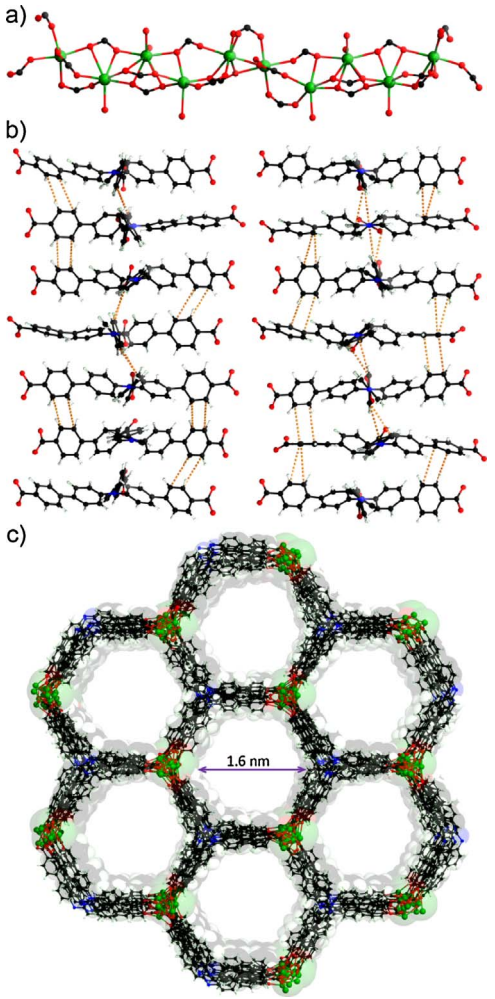

Fig. 1. (a) A Ca-COO chain running along the c axis; (b) Two parallel stacking arrays of TCPA fragments; (c) 3D framework showing nanoporous hexagonal channels.

3. Results and discussion

3.1. Crystal structure

The reaction of H_3TCPA and $Ca(NO_3)_2 \cdot 6H_2O$ in a mixed DMA/H_2O solvent at 120 °C for 3 days afforded the yellow triangular-prism-shaped crystals of **FIR-29**. Single-crystal X-ray diffraction analysis reveals that **FIR-29** crystallizes in a chiral space group $P3_121$. In each asymmetric unit, the five independent Ca^{2+} ions with the 6-, 7- or 8-coordinated geometries (Fig. 1a) are bridged by carboxyl groups to form a metallic pentamer $Ca_5(COO)_9$ and are further linked by three carboxyl groups in an ABBA··· arrangement, giving rise to an infinitely positive Ca-COO chain along the c axis. The TCPA ligands around the Ca-COO chain are closely arranged along the c direction, showing intermolecular interactions of consecutive long-range slipped π···π stacking with the distance between two C atoms from the phenyl rings of TCPA ligands measured at 3.5–3.8 Å (Fig. 1b) [50]. The favorable factor may support optimal electron or energy transfer process and endow desirable photocatalysis potential of **FIR-29**. In the structure of **FIR-29**, each rod-like Ca-COO chain is then connected to other six chains by long trigonal bridging ligand TCPA to form a 3D rod-packing architecture (Fig. 1c). Such rod-and-spacer approach has been proved